J. Phys. Chem. B **2006,** *110,* 22525−22531

Unsteady-State Direct Partial Oxidation of Methane to Synthesis Gas in a Fixed-Bed Reactor Using $AFeO_3$ (A = La, Nd, Eu) Perovskite-Type Oxides as Oxygen Storage

Xiao Ping Dai,[†,‡] **Ran Jia Li,**[‡] **Chang Chun Yu,***[,‡] **and Zheng Ping Hao***[,†]

Research Center for Eco-Environmental Science, Chinese Academy of Sciences,
Beijing 100085, People's Republic of China, and The Key Laboratory of Catalysis CNPC,
University of Petroleum, Beijing 102249, People's Republic of China

Received: June 6, 2006; In Final Form: August 19, 2006

Direct partial oxidation of methane to synthesis gas on $AFeO_3$ (A = La, Nd, Eu) oxides by a novel sequential redox cyclic reaction in the absence of gaseous oxygen was investigated over a fixed-bed reactor. These oxides were prepared by the sol−gel method and characterized by X-ray diffraction (XRD) and X-ray photoelectron spectroscopy (XPS) techniques. XRD analysis showed that all $AFeO_3$ (A = La, Nd, Eu) oxides, calcined at 1173 K, are single-phase perovskites. The CH_4-TPSR/MS and continuous reaction experiments indicated that the $AFeO_3$ (A = La, Nd, Eu) oxides provide mostly oxygen species, as the sole oxidant originated from lattice oxygen instead of gaseous oxygen, which can oxidize CH_4 to synthesis gas with high selectivity in the absence of gaseous oxygen. In terms of material economics and the amount of oxygen species for synthesis gas formation, the $LaFeO_3$ sample exhibits the best performance among these tested $AFeO_3$ oxides for synthesis gas production. The pulse experiments at different temperatures showed that the rate of oxygen migration during the CH_4 reaction with $LaFeO_3$ is strongly affected by the reaction temperature, and increases with rising temperature, which is favorable to much more CH_4 selective oxidation at high temperature. The two types of oxygen species are identified by experiments of continuous reactions and pulses, and confirmed by XPS. Methane can be converted selectively to synthesis gas by consumption of lattice oxygen, and general carbonaceous deposits on the catalyst surface do not occur under the appropriate reaction conditions by sequential redox cycles. The performance of selective oxidation of CH_4 to synthesis gas can be recovered by reoxidation using gaseous molecular oxygen; the $LaFeO_3$ oxide maintains relatively high catalytic activity and structural stability in redox atmospheres.

Introduction

The production of synthesis gas by steam reforming is a highly energy-consuming process, and about 60% of the cost of the overall chemical production process is due to synthesis gas generation by steam reforming.[1] Compared with conventional steam reforming, which requires high energy consumption and intensive capital, the partial oxidation of methane is more energy-efficient, requires a lower investment, and produces synthesis gas with a H_2/CO ratio of ca. 2, which is suitable for methanol and Fischer−Tropsch synthesis. Therefore, it has attained a lot of attention. However, partial oxidation of methane occurs between gas-phase oxygen and methane, which limits CO selectivity and hydrogen selectivity because of the complete oxidation of methane. There are also serious safety concerns due to the direct mixing of the highly explosive feed gas CH_4 with oxygen at high temperatures.[2] To avoid the above problems, intensive efforts have been made to use membrane reactors for the partial oxidation of methane to synthesis gas. In a membrane reactor, methane and air flow on opposite sides of the membrane, and methane is oxidized to CO/H_2 by lattice oxygen supplied from the air side of the membrane.[3] However, many practical problems such as reactor scale-up and sealing and engineering design still occur and should be solved before an industrial-scale implementation.[4]

A novel two-step process for the production of synthesis gas from methane and air has been recently proposed by Van Looij. Methane is oxidized to CO_2 and H_2O, which then reform methane for the production of synthesis gas in the absence of gas-phase oxygen by using a metal oxide acting as an oxygen storage.[5] Manganese, iron, and cerium oxides and cerium-containing mixed oxides have been studied, but poor thermal stability, carbon deposition, or sintering at high temperatures make it impossible to use them for practical application.[6−11]

Perovskite materials have been used quite effective for catalytic oxidation reactions including hydrogenation and hydrogenolysis of hydrocarbons, CO oxidation, ammonia oxidation, and catalytic combustion.[12] Due to their variable structure and chemical composition, much attention has been paid to perovskite-type oxides with a general formula ABO_3 (where A and B are usually rare earth and transition metal cations, respectively).[13] Perovskite oxides, which usually exhibit excellent redox properties, high oxygen mobility, and thermal stability, are good oxygen suppliers. However, the use of these materials for the direct conversion of methane to synthesis gas without gas-phase oxygen is rarely reported. In this work, a series of perovskite $AFeO_3$ oxides (A = La, Nd, Eu) are prepared and characterized, and their catalytic activities in the direct conversion of methane to synthesis gas in a fixed-bed reactor are investigated in the absence of gas-phase oxygen by

---

* Corresponding authors. Telephone: 86-10-89707447 (C.C.Y.); 86-10-62923564 (Z.P.H.). E-mail: lngcc@cup.edu.cn (C.C.Y.); zpinghao@rcees.ac.cn (Z.P.H.).

[†] Chinese Academy of Sciences.

[‡] University of Petroleum.

10.1021/jp063490b CCC: $33.50

TABLE 1: Tolerance Factor (t), Lattice Parameters (a, b, c), Interplanar Distance (d_{121}), and Average A−O and Fe−O Bond Distances of $AFeO_3$ (A = La, Nd, Eu) Oxides ($r(Fe^{3+}) = 0.645$ Å, $r(O^{2-}) = 1.4$ Å)

catalyst	A^{3+} ionic radius (Å)	tolerance factor	a (Å)	b (Å)	c (Å)	d_{121} (Å)	A−O (Å)	Fe−O (Å)
$LaFeO_3$	1.36	0.954	5.542	7.857	5.564	2.777	2.78	1.96
$NdFeO_3$	1.27	0.923	5.579	7.757	5.450	2.749	2.74	1.94
$EuFeO_3$	1.21	0.902	5.335	5.560	7.630	2.710	1.97	1.39

temperature programmed surface reaction, pulse reactions, continuous reactions, and sequential redox cycles. Catalysts with good performance and the reaction mechanism of oxygen species are desirable to be obtained.

Experimental Section

Material Preparation. The perovskite $AFeO_3$ oxide (A = La, Nd, Eu) catalysts were prepared by the sol−gel method. Glycine was added to an aqueous solution of metal nitrates to have a ratio $NH_3/NO_3 = 1.05$. Water was evaporated slowly from the mixed solution at 353−363 K until a viscous gel was obtained. The gel was then heated at 523 K for 30 min with a fast exothermic reaction, and the yielded brown powder precursor was slowly calcined at 1173 K for 10 h. The samples were crushed, ground, and sieved for experiment.

Material Characterization. Phase analysis and lattice parameters were performed by X-ray powder diffraction (XRD) using a ShiDU XRD-6000 with Ni-filtered Cu Kα radiation.

The X-ray photoelectron spectra were obtained with a VG ESCA LAB 210 system using Mg Kα radiation under ultrahigh vacuum (5×10^{-9} Pa). The spectra have been calibrated relatively to the C(1s) bond energy of contamination carbon, which was fixed at 284.6 eV.

Temperature Programmed Surface Reaction. Temperature programmed surface reaction with CH_4 (CH_4-TPSR/MS) was performed on a fixed-bed quartz microreactor (4.5 mm i.d.) packed with 0.2 g catalyst samples. In the TPSR experiments, the mixture of 11 vol % CH_4/Ar was used at a gas flow rate of 23 mL/min; linear temperature was increased at a rate of 10 K/min. The analysis of the reactants and products was carried out using an on-line mass spectrometer (AMTEK dycor System 1000), equipped with a fast response inlet capillary system. The quadrupole mass spectrometer can detect eight mass channels simultaneously with a minimum dwell time of 3 ms.

Pulse Reactions. The pulse reactions were performed by injecting in a carrier gas (Ar) flowing continuously through the catalyst bed. A pulse of CH_4 gas was introduced with a six-port gas-sampling valve equipped with measuring tubes (0.205 mL). The composition of the effluent gas from the reactor was monitored by a quadrupole mass spectrometer. The pulse measurements were carried out on catalyst (0.2 g) at 1173 K, with a carrier flow rate of 23 mL/min.

Continuous Reactions. Continuous reactions were carried out in a quartz microreactor. The $AFeO_3$ oxides were pretreated with 11% O_2/Ar at 23 mL/min at 1173 K for 30 min, and then flow of the reactant gas (11% methane in argon) at 23 mL/min was initiated and maintained for 4 min.

Sequential Redox Cycles. Sequential redox cycles over $LaFeO_3$ oxide were performed in a fixed-bed reactor for the production of synthesis gas at 1173 K between reductive (CH_4/He) and oxidative atmospheres (O_2/Ar) (denoted as “redox”). The total gas flow rate was kept at 23 mL/min. Ar/He was used as dilution gas and tracer gas.

The different reaction products were continuously measured with the mass spectrometer at $m/e = 2$ (H_2), $m/e = 15$ (CH_4), $m/e = 18$ (H_2O), $m/e = 28$ (CO), $m/e = 32$ (O_2), and $m/e = 44$ (CO_2). The CH_4, CO, H_2, and CO_2 pulses were injected in order to calculate the amount of CH_4, CO, and CO_2 on the catalysts taking into account a previous calibration of the mass spectrometer. The calibration of the mass spectrometer was carried out with standard mixtures of known composition. The cracking coefficients of methane, CO, and CO_2 have been determined and used to calculate their concentrations. The CO selectivity is defined as $CO/(CO + CO_2) \times 100\%$.

Results and Discussion

Material Characterizations. A perovskite-type oxide has an ABO_3-type crystal structure wherein cations with a large ionic radius have 12 coordination to oxygen atoms and occupy A-sites, and cations with a smaller ionic radius have 6 coordination and occupy B-sites. The ionic radii of the two cations A and B in a perovskite structure (ABO_3) compound must be in a limited range, i.e., $r_A > 0.090$ nm and $r_B > 0.051$ nm. The tolerance factor of the perovskite compound t ($t = (r_A + r_O)/\sqrt{2}(r_B + r_O)$) should be in the range of 0.8−1.0.[14]

The tolerance factor (t) values calculated by the above equation are listed for $AFeO_3$ (A = La, Nd, Eu) oxides in Table 1. It is seen that all tolerance factor (t) values of the $AFeO_3$ (A = La, Nd, Eu) oxides are in the range of 0.8−1.0. Thus, it is possible for these oxides with stoichiometric composition to form a single perovskite phase.

The XRD spectra of $AFeO_3$ (A = La, Nd, Eu) samples calcined at 1173 K are shown in Figure 1. The results show that $AFeO_3$ (A = La, Nd, Eu) samples are single-phase perovskites, compared with the XRD data of the perovskite-structure $AFeO_3$ oxide (JCPDS Card Nos. 37-1498, 25-1149, and 47-0066, respectively). It is notable that the crystallinity of the samples is much higher for $LaFeO_3$ and lower for $NdFeO_3$ and $EuFeO_3$. Also, Figure 1 clearly shows that the X-ray lines are continuously shifted toward higher diffraction angles with the decrease of the A ionic radii.

Table1 lists the observed values of lattice parameters and the average A−O and Fe−O bond distances for $AFeO_3$ (A = La,

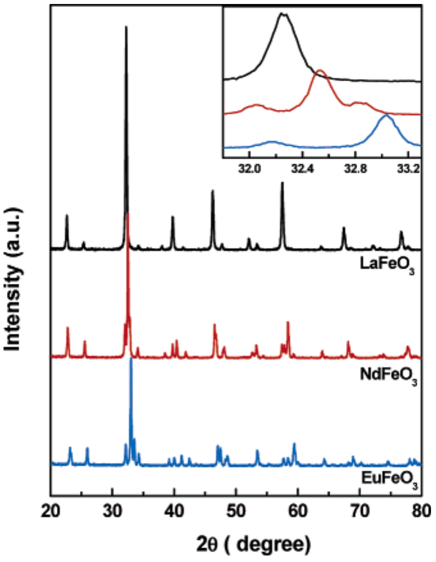

Figure 1. XRD spectra for $AFeO_3$ (A = La, Nd, Eu) samples calcined at 1170 K.

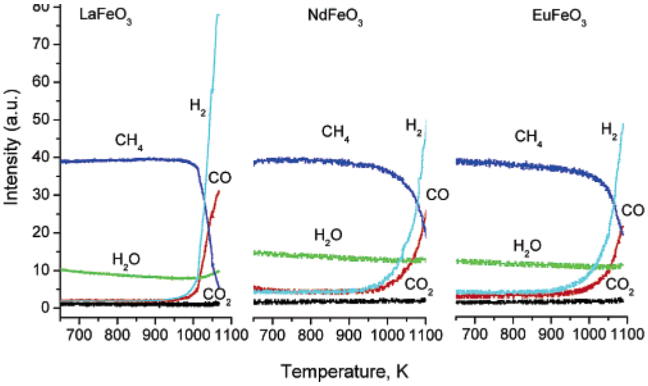

Figure 2. CH_4-TPSR/MS profiles in 11% CH_4/Ar over $AFeO_3$ oxides.

Nd, Eu) samples. As seen, lattice symmetry changes from orthorhombic to nearly cubic in the series $EuFeO_3 \rightarrow NdFeO_3 \rightarrow LaFeO_3$. The lattice parameter *c* in $LaFeO_3$ approaches the value of *a*, and *b* is equal to the double length of the cubic pseudocell dimension. The average A−O and Fe−O bond distances were evaluated by taking into account half the value of *b* as the cell dimension of the idealized cubic unit cell (A−O $= b\sqrt{2}/4$, Fe−O $= b/4$).[15]

The values of unit cell parameters of $LaFeO_3$, $NdFeO_3$ and $EuFeO_3$ are similar to those reported in the literature.[15,16] The Fe−O bond is slightly stronger in $EuFeO_3$ than in $LaFeO_3$ and $NdFeO_3$; the Fe−O bond strength should be considered to be related to catalytic performance and the chemical structure of $AFeO_3$ (A = La, Nd, Eu) oxides. The interplanar distance (d_{121}) increases with the increase of A^{3+} ionic radii, resulting in the increase of the Fe−O bond distance, which is related to the electronic structure of A-site cation.

Temperature Programmed Surface Reaction (CH_4-TPSR/MS). Figure 2 shows a variation of product formation and methane conversion as a function of reaction temperature during CH_4-TPSR/MS over the $AFeO_3$ (A = La, Nd, Eu) oxides.

It was shown that the main products are CO and H_2. Only small amounts of CO_2 and H_2O were detected over the $AFeO_3$ (A = La, Nd, Eu) oxides. This demonstrates that the $AFeO_3$ (A = La, Nd, Eu) oxides provide mainly oxygen species, which can oxidize CH_4 to CO/H_2 with high selectivity, and only a small quantity of methane was oxidized to CO_2. No reaction was monitored over $AFeO_3$ (A = La, Nd, Eu) oxides below 860 K; greater CH_4 conversion took place in CH_4-TPSR on $AFeO_3$ (A = La, Nd, Eu) oxides above 1000 K. Obviously the amount of oxygen cannot be ascribed to only the surface oxygen, because of the amount of oxygen at the first surface layer on the basis of low BET surface area (ca. 10 m^2/g oxide calcined at 1173 K). Therefore, it is clear that the bulk lattice oxygen of $LaFeO_3$ oxide should participate in the partial oxidation of CH_4 to synthesis gas. The oxygen species are transported by the surface reaction and bulk ion conduction mechanism. It should be noted that in Figure 2 the diffusion rates of oxygen have obvious differences due to the various gradients of the CO and H_2 formation curves. The diffusion rate of oxygen has the highest value in $LaFeO_3$ oxide according to the gradients of CO formation curves. The amounts of CO and H_2 are higher on $LaFeO_3$ oxide than on $NdFeO_3$ and $EuFeO_3$ oxides, and this indicates that the amount of oxygen species for synthesis gas formation is the highest in $LaFeO_3$ oxide, as shown in Table 2. This behavior reflects the increase in Fe−O bond strength deduced from bond distance considerations and confirms the major role of lattice oxygen species in partial oxidation of methane. The B−O bond energy lowers with the decrease of the tolerance factor.[17] This proves the easier oxygen mobility for a high tolerance factor of perovskite oxide, such as $LaFeO_3$ oxide.

TABLE 2: O Species Amounts for CH_4 Oxidation

catalyst	less reactive O species[a] μmol/g catalyst	very reactive O species[a] μmol/g catalyst	O species amt for CO formation[b] μmol/g catalyst
$LaFeO_3$	669.0	242.2	346.0
$NdFeO_3$	422.5	504.8	286.4
$EuFeO_3$	368.0	184.0	266.7

[a] Continuous reactions at 1173 K. [b] CH_4-TPSR/MS.

Continuous Reactions over $AFeO_3$ Oxides. The methane oxidation experiments shown here are inherently transient since the oxidation level of the solid declines with the consumption of lattice oxygen. The duration of flow experiments was therefore, limited to 4 min in all runs.

Transient product concentrations for the reaction of 11% CH_4/Ar at 1173 K on $AFeO_3$ (A = La, Nd, Eu) oxides are shown in Figure 3. Figure 3a indicates that the reactions were initially very fast and produced significant quantities of carbon dioxide and water but not the desired products (carbon monoxide and hydrogen) at the preliminary stage. When the surface state was changed, carbon dioxide and water formation declined rapidly to a very low level, while methane intensity quickly declined, which means that methane conversion was sharply enhanced. With the surface oxygen species consumed, CO and H_2 intensities increased steadily with time, while the CH_4 intensity decreased gradually, and the synthesis gas was the dominant product. After 60 s of reaction in CH_4/Ar, the intensities of CH_4, H_2, and CO reached steady-state levels. The delay was observed in the appearance of CO_2 and the other products (such as CO and H_2), indicating that, in the absence of gas-phase oxygen, methane first reacted with the very reactive oxygen species to form CO_2 and H_2O. After these oxygen species declined, the less reactive oxygen species reacted selectively with methane to form CO and H_2. From the trend of the methane intensity change, it was noted that the consumption of lattice oxygen on surface enhances oxygen mobility from the bulk toward the surface. Exposure of $LaFeO_3$ oxides to a reduced atmosphere can generate oxygen vacancies, owing to the loss of lattice oxygen and reduction of oxidation state of the Fe ion simultaneously.[18] Similarly, Tejuca[19] reported the reduction of Fe^{3+} to Fe^{2+} and further to metallic Fe in $LaFeO_3$ oxide.

After the reductive reaction with methane, the catalyst was reoxidized by 11 mol % O_2/Ar for 4 min at 1173 K isothermal

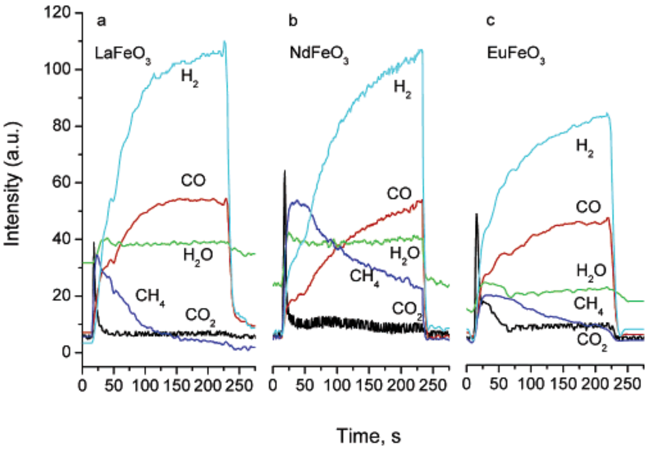

Figure 3. Responses of the transient from Ar to 11 mol % CH_4/Ar over $AFeO_3$ oxides at 1173 K.

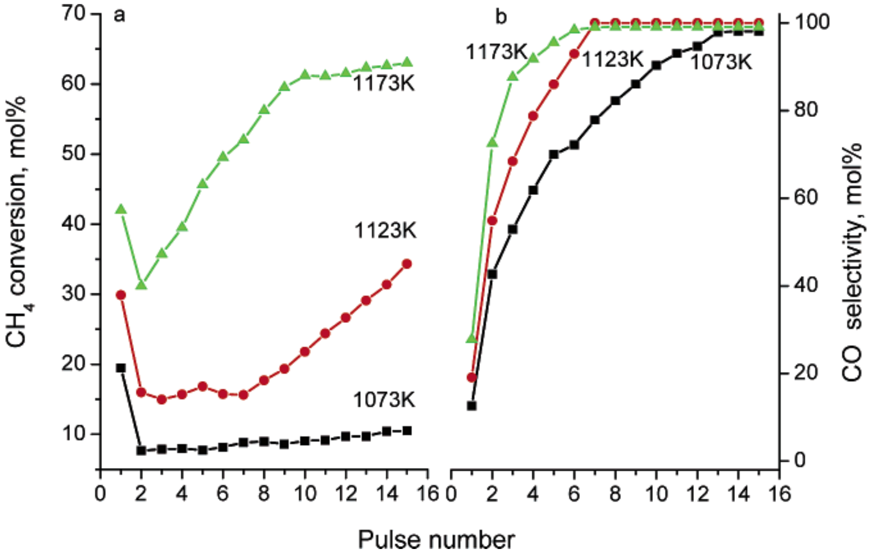

Figure 4. 4: CH_4 conversion and CO selectivity vs temperature of pulse reaction over $LaFeO_3$ oxide.

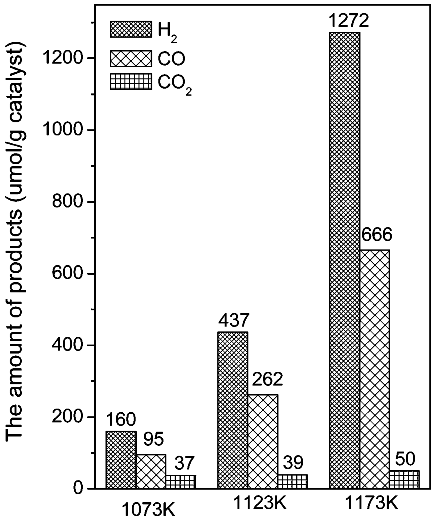

Figure 5. Total amount of products in 15 pulse reactions over $LaFeO_3$ oxide at different temperatures.

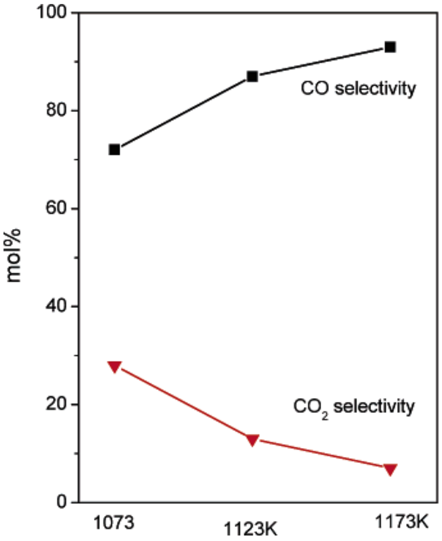

Figure 6. Total CO selectivity and CO_2 selectivity in 15 pulse reactions over $LaFeO_3$ oxide at different temperatures.

conditions. In the first 90 s, no oxygen was detected in the effluent gas. The oxygen storage on oxides was recovered very efficiently. During the reoxidation step, the signal of CO_2 and CO was not detected over $LaFeO_3$ oxide, which implies that almost no carbon was deposited on the oxides during the methane reaction step under the reaction conditions.

The same trend occurred over $NdFeO_3$ and $EuFeO_3$ oxides as shown in Figure 3b,c. The comparison of the catalytic behaviors for the three oxides indicates that the $NdFeO_3$ and $EuFeO_3$ oxides exhibit lower methane conversion, are less selective for synthesis gas, and produce substantial quantities of carbon dioxide and water. From the gradients of CO and H_2 profiles, it can be seen that the diffusion rate of lattice oxygen from the bulk toward the surface is lower over $NdFeO_3$ and $EuFeO_3$ oxides than over $LaFeO_3$ oxide. The O species amount for CH_4 oxidation is shown in Table 2. The maximum value of less reactive oxygen species released by $LaFeO_3$ oxide confirms its best catalytic performance for synthesis gas formation. This agrees with the results in CH_4-TPSR experiments.

In terms of economics of material, considering the amount of selective oxygen species and the diffusion rate of lattice oxygen from the bulk toward the surface, the $LaFeO_3$ sample exhibits the best performance among these tested $AFeO_3$ oxides for synthesis gas production in CH_4-TPSR and continuous reactions. Therefore, it is deduced that $LaFeO_3$ is the best catalyst among the tested $AFeO_3$ oxides, so it was chosen for in-depth study.

Pulse Reactions over $LaFeO_3$ Oxide at Different Temperatures. The reactor temperature was raised under oxygen flow, and a sweeping step with inert gases was carried out before the pulse reaction. The results of catalytic tests carried out by pulse reaction with CH_4/Ar in the absence of gas-phase oxygen are presented in Figures 4−6 for $LaFeO_3$ oxide at different temperatures.

For different temperatures, the reaction started with relatively high conversion of methane in the first pulse, i.e., 20% for 1073 K and 42% for 1173 K (Figure 4a). Afterward, there was a sharp decline of methane conversion from pulse 1 to pulse 2, and a quick increase thereafter. On the other hand, the carbon monoxide selectivity rose sharply from a very low level to above 90% within the first few pulses. There are pronounced differences between different temperatures. Higher temperature gives a higher initial methane conversion and higher carbon monoxide selectivity (Figure 4b). CH_4 conversion and CO selectivity increase with reaction temperature; especially the tendency is sharper at high reaction temperatures. From Figures 5 and 6,

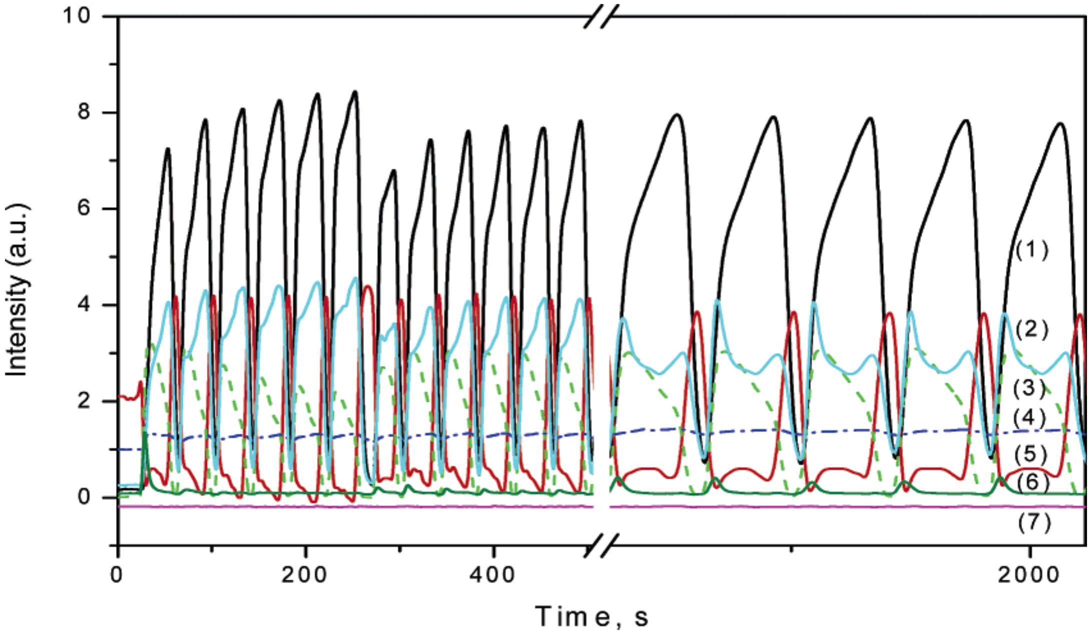

Figure 7. Transient responses of the cyclic reaction between O_2/Ar flow (10 s) and CH_4/He flow (30 s) over $LaFeO_3$ oxide at 1173 K: 1, H_2; 2, CO; 3, CH_4; 4, H_2O; 5, Ar; 6, CO_2; 7, O_2.

the total amounts of CO and H_2 increased sharply when the reaction temperature was increased from 1073 to 1173 K, due to the higher diffusion rate at high temperature. The total selectivity of CO increased with reaction temperature, and much more of CH_4 was selectively oxidized to CO and H_2 at high temperatures.

The explanation could be that first CO_2 is likely produced by the reaction between methane and the chemisorbed oxygen species on oxide.[20] After the concentrations of surface oxygen species decline, lattice oxygen is diffused from the bulk to the surface when the pulse reaction of CH_4 is carried out continuously. With the oxygen species on the surface of $LaFeO_3$ oxide consumed, the increased concentration of lattice oxygen vacancies provides pathways of oxygen transport through the lattice, and leads to enhancement of oxygen diffusivity. It is well-known that oxygen vacancies can be formed easily when a perovskite is heated at higher temperature. The migration rate of oxygen during the CH_4 reaction with $LaFeO_3$ oxide was strongly affected by the reaction temperature, especially at high reaction temperatures. The rate of oxygen migration from the bulk to the surface increased with rising temperature, and more CO and H_2 could be formed due to selective oxidation of CH_4. The difference in CH_4 conversion at different temperatures is due to the high activation energy of the activated oxygen, which implies the importance of the collective properties of perovskites, e.g., the bond energy of the lattice oxygen.[21]

Production of Synthesis Gas by Sequential Redox Cycles over $LaFeO_3$. The oxidation of hydrocarbons is supposed to occur on the perovskite surface by means of an intrafacial catalytic mechanism, in which the adsorbed oxygen is partly consumed and regenerated during a continuous cycle.[4,22,23] DuPont commercialized a circulating fluidized bed concept in which catalyst is shuttled between a net oxidizing and a net reducing environment.[24] Sequential redox cycles were carried out in a fixed-bed reactor for the production of synthesis gas over $LaFeO_3$ oxide catalyst at 1173 K between O_2/Ar (11 mol % O_2) and CH_4/He (11 mol % He). The total gas flow rate was kept at 25 mL/min. Ar/He was used as dilution gas and tracer gas. Related results are shown in Figures 7 and 8.

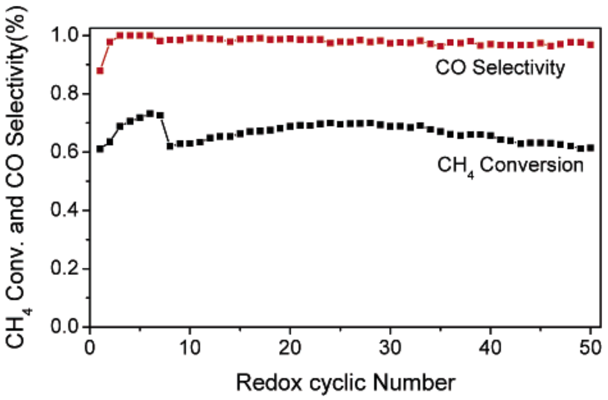

Figure 8. CH_4 conversion and CO selectivity as a function of redox cycle number.

Figure 7 shows the product responses during the cyclic reactions between O_2/Ar oxidation for 10 s and CH_4/He reduction for 30 s over the $LaFeO_3$ catalyst at 1173 K. As described previously (Figure 3a), CO_2 was formed first and then CO and H_2 were detected for the first cycle. However, from the second redox cycle to the sixth redox cycle, only a small quantity of CO_2 was produced, while CO and H_2 were the dominant products. Fe^{4+} was present in small amounts also in the $LaFeO_3$ perovskite, and partial reduction of Fe^{4+} to Fe^{2+}, Fe^{3+} to Fe^{2+} could likely occur at higher temperature even if it does not lead to the loss of the perovskite structure.[15] It has also been reported that, once the reaction temperature exceeded 1173 K, the sintering of iron oxide occurred.[25] With the increase of cycle number from the seventh redox cycle, the amount of CO_2 increased, which may be due to the change of the redox properties of Fe. From the 50 redox cycles at 1173 K, the $LaFeO_3$ oxide maintained relatively high catalytic activity and structural stability in XRD characterization (shown in Figure 9), but the products provide evidence of the appearance of deactivation phenomena (shown in Figure 8). When the lattice oxygen consumed at reductive atmospheres (CH_4/He) is not sufficiently restored at oxidative atmospheres for 10 s, the oxidation level of the catalyst may not reach the initial state,

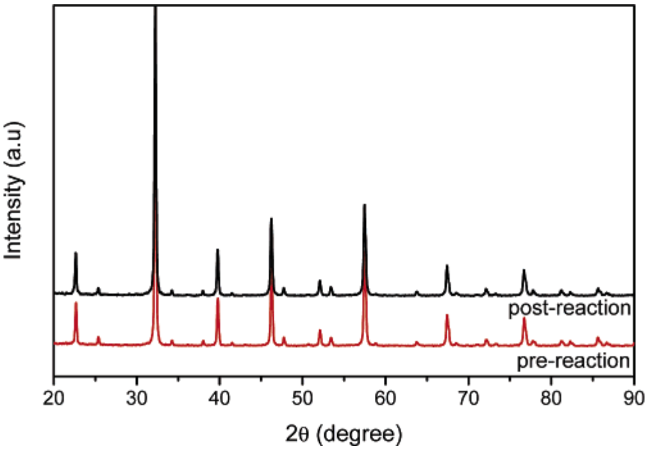

Figure 9. Comparison of XRD profiles over pre- and postreaction $LaFeO_3$ catalyst.

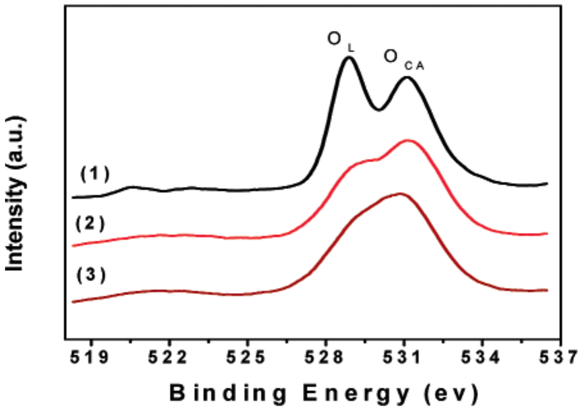

Figure 10. XPS of O(1s) over pre- and postreaction $LaFeO_3$ oxides: 1, prereaction oxide; 2, postreaction oxide (75 s in 11% CH_4/Ar); 3, postreaction oxide (180 s in 11% CH_4/Ar).

but the most reactive oxygen species can be recovered. They can react with CH_4 to form synthesis gas. The results of catalyst reoxidation in the redox cycle indicate that the oxide has a high reactivity toward the oxygen and the oxygen can be consumed completely. It should be noted that no CO_2 and CO were observed, which could result from the oxidation of carbonaceous deposits on the catalyst surface by O_2/Ar. This indicates that methane pyrolysis does not occur at the appropriate reaction condition. The ratio of H_2/CO is about 1.93 and near the stoichiometric ratio of the partial oxidation of methane.

Figure 8 shows the variations of CH_4 conversion and selectivity for CO as a function of redox cycles. The $LaFeO_3$ oxide exhibits better catalytic activity for the production of synthesis gas. The CH_4 conversions depend on the cycle number and remain at high level of 60−70%, but decrease slightly with the increase of cycle number, while the selectivities to CO with the increase of the cycle number and remain at higher level (>96%). This indicates that oxygen species for the CO formation can be recovered, while the reactive oxygen species for the CO_2 formation is hardly restored at the appropriate condition.

Surface Oxygen Species of $LaFeO_3$ Oxides. It is well-known that the surface oxygen species play an important role in the catalytic oxidation reaction. XPS measurements were performed on pre- and postreaction $LaFeO_3$ oxides, as shown in Figure 10.

The oxides were pretreated by switching to CH_4/Ar for 75 and 180 s at 1173 K and then changing to He for cooling to room temperature. The XPS analysis of the O(1s) core level spectra shows that it is composed of two peaks, indicating two types of oxygen presented on the pre- and post-reaction $LaFeO_3$ oxide surface. These two oxygen species can be defined as a very reactive oxygen species for the CO_2 formation and a less reactive oxygen species for the synthesis gas formation. The line at ca. 528.9 eV is assigned to the oxygen in the lattice, and the one at ca. 531.1 eV is assigned to adsorbed oxygen containing species.[26−28] Omata et al.[29] reported that two kinds of oxygen species existed in substituted $SrCoO_3$ perovskite, and they are responsible for selective oxidation and complete oxidation, respectively. This is in agreement with the results of our experiments. It is clear that the lattice oxygen decreases after reacting with 11 mol % CH_4/Ar at 1173 K. The prereaction oxide has a higher value of O_{lat}/O_{ads} (ca. 0.74) than the postreaction oxide (ca. 0.49) on the surface, and the value of O_{lat}/O_{ads} decreases from 0.58 to 0.49 with the reaction time increased from 75 to 180 s with 10% CH_4/Ar. The different amounts of the lattice oxygen indicate that the oxygen vacancies increase due to the reaction with methane. The amount of adsorbed oxygen containing species is difficult to determine since the oxides are inevitable owing to contact with air. This is consistent with the results obtained from unsteady-state reactions, which indicate CO_2 formation first and then CO production. As Voorhoeve et al. proposed,[23] two different mechanisms of catalytic oxidation should be distinguished: (i) a suprafacial process in which the catalyst surface provides a set of electronic orbitals of proper symmetry and energy for the bonding of reactants and intermediates, and (ii) intrafacial reactions in which the catalyst participates as a reagent that is partly consumed and regenerated in a continuous cycle. In the former mechanism, the oxygen vacancies at the catalyst surface play a relevant role for the adsorption and activation of the reactant molecules, whereas in the latter mechanism, the metal cation of the catalyst oxide should have the capacity to change the oxidation state and thus to participate in a redox cycle.

Conclusions

A novel sequential redox cyclic reaction for methane partial oxidation to synthesis gas is reported using perovskite-type oxides as oxygen storage free of gaseous oxygen. Based on the redox cyclic reaction, $AFeO_3$ oxides (A = La, Nd, Eu) were prepared via the sol−gel method and identified by their XRD patterns. All $AFeO_3$ (A = La, Nd, Eu) oxides, calcined at 1173 K, are single-phase perovskites. The Fe−O bond is affected by A^{3+} ionic radii, which could be related to the catalytic activity of partial oxidation of methane. From the CH_4-TPSR/MS experiments, the $AFeO_3$ (A = La, Nd, Eu) oxides provide mostly oxygen species, which can oxidize CH_4 to synthesis gas with high selectivity.

The investigation of the continuous reaction of CH_4 oxidation at 1173 K in the absence of gas-phase oxygen indicates that methane was reacted first with the very reactive oxygen species to form CO_2, and then the less reactive oxygen species reacted selectively with methane to form CO and H_2. $AFeO_3$ (A = La, Nd, Eu) oxides are the only oxygen source in the oxidation of CH_4 to synthesis gas. The $LaFeO_3$ sample has the highest selectivity to synthesis gas, and it is the best catalyst among the tested $AFeO_3$ oxides for synthesis gas production.

The pulsed experiments at different temperatures imply that the rate of oxygen supply during the CH_4 reaction with $LaFeO_3$ oxide was strongly influenced by the reaction temperature. Two types of oxygen species are present on the $LaFeO_3$ oxides, and they are responsible for CO_2 formation and synthesis gas formation. The rate of oxygen migrating from the bulk to the surface increases with an increase in temperature, and more CH_4

is selectively oxidized to CO and H_2. The synthesis gas production prefers to occur over the $LaFeO_3$ oxide at high temperature.

Methane can be converted selectively to synthesis gas, which is suitable for Fischer–Tropsch synthesis, under the appropriate reaction conditions by redox cycles. The property of selective oxidation of CH_4 to synthesis gas can be recovered by reoxidation using gaseous molecular oxygen. The $LaFeO_3$ oxide maintained relatively high catalytic activity and structural stability in redox atmospheres. The results clearly indicate that the partial oxidation of methane over $LaFeO_3$ proceeds via a suprafacial process and intrafacial reaction mechanism as Voorhoeve et al. proposed.

Acknowledgment. Financial support from the Chinese Natural Science Foundation (Project Nos. 20306016 and 20322201) and the National Basic Research Program of China (2004CB217808, 2004CB719500) is gratefully acknowledged.

References and Notes

(1) Haggin, J. *Chem. Eng. News* **1990**, *23*, 27.
(2) Vanderstraeten, B.; Tuerlinckx, D.; Berghmans, J.; Vligen, S.; Van't Oost, E.; Smit, B. *J. Hazard. Mater.* **1997**, *56*, 237.
(3) Pantu, P.; Kim, K.; Gavalas, G. R. *Appl. Catal., A* **2000**, *193*, 203.
(4) Zeng, Y.; Tamhankar, S.; Ramprasad, N.; Fitch, F.; Acharya, D.; Wolf, R. *Chem. Eng. Sci.* **2003**, *58*, 577.
(5) Van Looij, F.; Van Giezen, J. C.; Stobbe, E. R. *Catal. Today* **1994**, *21*, 495.
(6) Stobbe, E. R.; de Boer, B. A.; Geus, J. W. *Catal. Today* **1999**, *47*, 161.
(7) Li, R. J.; Yu, C. C.; Dai, X. P.; Shen, S. K. *Chin. J. Catal.* **2002**, *23*, 381.
(8) Trovarelli, A.; de Leitenburg, C.; Dolcetti, G. *CHEMTECH* **1997**, *27*, 32.
(9) Otsuka, K.; Wang, Y.; Sunada, E.; Yananaka, I. *J. Catal.* **1998**, *175*, 152.
(10) Fornasiero, P.; Balducci, G.; Di Monte, R.; Ka<crn>spar, J.; Sergo, V.; Gubitosa, G.; Ferrero, A.; Graziani, M. *J. Catal.* **1996**, *164*, 173.
(11) Otsuka, K.; Wang, Y.; Nakamura, M. *Appl. Catal., A: Gen.* **1999**, *183*, 317.
(12) O'Connell, M.; Norman, A. K.; Hüttermann, C. F.; Morris, M. A. *Catal. Today* **1999**, *47*, 123.
(13) Porta, P.; Cimino, S.; Rossi, S. D.; Faticanti, M.; Minelli, G.; Pettiti, I. *Mater. Chem. Phys.* **2001**, *71*, 165.
(14) Burggraaf, A. J.; Cot, L. *Fundamentals of Inorganic Membrane Science and Technology*; Elsevier: Amsterdam, 1996; p 435.
(15) Ciambelli, P.; Cimino, S.; Rossi, S. D.; Lisi, L.; Minelli, G.; Porta, P.; Russo, G. *Appl. Catal., B* **2001**, *29*, 239.
(16) Niu, X. S.; Du, W. M.; Du, W. P. *Sens. Actuators, B* **2004**, *99*, 399.
(17) Voorhoeve, R. J. H.; Burton, J. J.; Garton, R. L. *Advanced Materials in Catalysis*; Academic Press: New York, 1977; p 129.
(18) Ramos, T.; Atkinson, A. *Solid State Ionics* **2004**, *170*, 275.
(19) Tejuca, L. G.; Fierro, J. L. G.; Tasćon, J. M. D. *Adv. Catal.* **1989**, *36*, 237.
(20) Machida, M.; Eguchi, K.; Arai, H. *J. Catal.* **1990**, *123*, 477.
(21) Ciambelli, P.; Cimino, S.; Lasorella, G.; Lisi, L.; Rossi, S. D.; Faticanti, M.; Minelli, G.; Porta, P. *Appl. Catal., B* **2002**, *37*, 231.
(22) Seiyama, T. *Catal. Rev.–Sci. Eng.* **1992**, *34*, 281.
(23) Voorhoeve, R. J. H.; Remeika, J. P.; Trimble, L. E. *Ann. N. Y. Acad. Sci.* **1976**, *272*, 3.
(24) Contractor, R. M.; Garnett, D. I.; Horowitz, H. S.; Bergna, H. E.; Patience, G. S.; Schwartz, J. T.; Sisler, G. M. In *New Development in Selective Oxidation II*; Corberan, C., Bellon, S. V., Eds.; Elsevier: Amsterdam, 1994; p 233.
(25) Li, R. J.; Shen, S. K. *J. Mol. Catal. (China)* **2001**, *15*, 181.
(26) Tavares, A. C.; da Silva Pereira, M. I.; Mendonça, M. H.; Nunes, M. R.; Costa, F. M.; Sá, C. M. *J. Electroanal. Chem.* **1998**, *449*, 91.
(27) Haenen, J.; Visscher, W.; Barendrecht, E. *J. Electroanal. Chem.* **1986**, *208*, 297.
(28) Alifanti, M.; Kirchnerova, J.; Delmon, B. *Appl. Catal., A* **2003**, *245*, 231.
(29) Omata, K.; Yamazaki, O.; Tomita, K.; Fujimoto, K. *J. Chem. Soc., Chem. Commun.* **1994**, 1647.